Computer Physics Communications 185 (2014) 323–329

Contents lists available at ScienceDirect

Computer Physics Communications

journal homepage: www.elsevier.com/locate/cpc

carlomat, version 2 of the program for automatic computation of lowest order cross sections☆

Karol Kołodziej*

Institute of Physics, University of Silesia, ul. Uniwersytecka 4, PL-40007 Katowice, Poland

ARTICLE INFO

Article history:
Received 16 May 2013
Received in revised form
18 July 2013
Accepted 26 August 2013
Available online 4 September 2013

Keywords:
Automatic calculation of cross sections
Monte Carlo
Extensions of standard model

ABSTRACT

Version 2 of carlomat, a program for automatic computation of the lowest order cross sections of multiparticle reactions, is described. The substantial modifications with respect to version 1 of the program include: generation of a single phase space parameterization for the Feynman diagrams of the same topology, an interface to parton density functions, improvement of the color matrix computation, the Cabibbo–Kobayashi–Maskawa mixing in the quark sector, the effective models including scalar electrodynamics, the *Wtb* interaction with operators of dimension up to 5 and a general top–Higgs coupling. Moreover, some minor modifications have been made and several bugs in the program have been corrected.

Program summary

Program title: carlomat, version 2.0

Catalogue identifier: AEDQ_v2_0

Program summary URL: http://cpc.cs.qub.ac.uk/summaries/AEDQ_v2_0.html

Program obtainable from: CPC Program Library, Queen's University, Belfast, N. Ireland

Licensing provisions: Standard CPC licence, http://cpc.cs.qub.ac.uk/licence/licence.html

No. of lines in distributed program, including test data, etc.: 49058

No. of bytes in distributed program, including test data, etc.: 25748755

Distribution format: tar.gz

Programming language: Fortran 90/95

Computer: All

Operating system: Linux

Classification: 4.4, 11.2

Catalogue identifier of previous version: AEDQ_v1_0

Journal reference of previous version: Comput. Phys. Comm. 180 (2009) 1671

Does the new version supersede the previous version?: Yes

Nature of problem:
Leading order predictions for reactions of two particle scattering into a final state with up to 10 particles within the Standard Model and some effective models.

Solution method:
As in version 1 of the program, the matrix element in the helicity basis and multichannel Monte Carlo phase space integration routine are generated automatically for a user specified process. The color matrix is divided into smaller routines and written down as a stand alone program that is calculated prior to compilation and execution of the Monte Carlo program for computation of the cross section. The phase space integration routine is substantially shortened in order to speed up its compilation. The

☆ This paper and its associated computer program are available via the Computer Physics Communication homepage on ScienceDirect (http://www.sciencedirect.com/science/journal/00104655).

* Tel.: +48 32 3591834; fax: +48 32 2588431.
E-mail address: karol.kolodziej@us.edu.pl.

http://dx.doi.org/10.1016/j.cpc.2013.08.023

code generation part of the program is modified to incorporate the scalar electrodynamics and effective Lagrangians of the top quark interactions with the W and Higgs bosons. Routines necessary for computing the helicity amplitudes of new couplings are added.

Reasons for new version:
The main reasons for the revision are:

1. To adjust the program for the description of hadron collisions.
2. To facilitate computation of the color matrix that is usually much more involved for processes of the hadron–hadron collision than for processes of electron–positron annihilation.
3. To shorten compilation time of the generated kinematical routines.
4. To implement some extensions of the standard model in the program.

Summary of revisions:
A few substantial modifications are introduced with respect to version 1.0 of the program. First, a single phase space parameterization is generated for the Feynman diagrams of the same topology taking into account possible differences in mappings of peaks in the individual diagrams, which speeds up a compilation time of the Monte Carlo program for multiparticle reactions by a factor 4–5 with respect to the previous version. Second, an interface to parton density functions is added that allows predictions to be made for hadron collisions. Third, calculation of the color matrix is facilitated. Fourth, the Cabibbo–Kobayashi–Maskawa mixing in the quark sector is implemented. Fifth, the effective models including scalar electrodynamics, the Wtb interaction with operators of dimension up to 5 and a general top–Higgs coupling are implemented. Moreover, some minor modifications have been made and several bugs in the program have been corrected.

Restrictions:
Although the compilation time has been shortened in the current version, it still may be quite long for processes with 8 or more final state particles. Another limitation is the size of the color matrix that, if too big, may prevent compilation or result in a very long execution time of the color compilation program. This actually may happen already for some QCD processes with 7 partons such as $gg \to 5g$, the commutation time of the color matrix of which, is about 200 h.

Running time:
Depends strongly on the selected process and, to a lesser extent, on the Fortran compiler used. The following amounts of time are needed at different computation stages of the top quark pair production parton level process $gg \to bu\bar{d}\,\bar{b}\mu^-\bar{\nu}_\mu$, to produce the appended test output files on a PC with the Pentium 4 3.0 GHz processor with Absoft (GNU, Intel) Fortran compilers: code generation takes 3.7 s (3.7 s, 2.4 s), compilation, computation and simplification of the color matrix takes about 1 s (1 s, 1 s), compilation of all the generated routines takes just a few seconds and execution of the Monte Carlo program takes about 44 s (41 s, 23 s).

1. Introduction

In the era of the LHC, production of a few heavy particles such as the electroweak (EW) gauge bosons, top quark or recently discovered scalar candidate for the Higgs boson, at a time have become commonplace. The heavy particles live so briefly that they should be actually regarded as the intermediate states of reactions with multiple light particles in the final state. As an example consider

$$gg \to bu\bar{d}\,\bar{b}\mu^-\bar{\nu}_\mu, \tag{1}$$

$$u\bar{u} \to bu\bar{d}\,\bar{b}\mu^-\bar{\nu}_\mu \tag{2}$$

which are underlying partonic processes of the top quark pair production in the proton–proton collisions at the LHC, $pp \to t\bar{t}$. The final state of (1) and (2) corresponds to each of the top quarks decaying into a b-quark and a W-boson and, subsequently one of the W bosons decaying leptonically and the other hadronically, as depicted in Figs. 1(a), (b), 2(a) and (b). However, both reactions receive contributions from many other Feynman diagrams which do not represent the signal of the top quark pair production. Some examples of such diagrams are depicted in Fig. 1(c)–(f) for reaction (1) and in Fig. 2(c)–(d) for reaction (2). The entire number of the leading order Feynman diagrams of reactions (1) and (2) in the unitary gauge of the standard model (SM), with the neglect of the Higgs boson coupling to fermions lighter than the b-quark and of the Cabibbo–Kobayashi–Maskawa (CKM) mixing amounts to 421 and 718, respectively.

Another example is

$$gg \to bu\bar{d}\bar{b}\mu^-\bar{\nu}_\mu b\bar{b} \tag{3}$$

that is a dominant partonic process of the associated production of the top quark pair and Higgs boson in the proton–proton collisions at the LHC, $pp \to t\bar{t}h$, where one of the top quarks decays hadronically, the other semileptonically and the Higgs boson decays into the $b\bar{b}$-pair, as depicted in Fig. 3(a)–(c). The diagrams depicted in Fig. 3(d)–(f) are examples of the background contributions to associated production of the Higgs boson and top quark pair. Under the same assumptions as above, the entire number of Feynman diagrams is equal to 67 300.

It is needless to say that reliable theoretical predictions for reactions such as (1)–(3) can be obtained only within a fully automated approach, as offered by, e.g., `carlomat` [1], but it should also be possible to solve the problem at hand with any other of the following general purpose packages for Monte Carlo (MC) simulations: `MadGraph/MadEvent/HELAS` [2], `CompHEP/CalcHEP` [3], `ALPGEN` [4], `HELAC-PHEGAS` [5], `SHERPA/Comix` [6] and `OMega/Whizard` [7], or the programs for calculating NLO EW or QCD corrections to scattering amplitudes such as `FeynArts/FormCalc` [8], `GRACE` [9] and `HELAC-NLO` [10]. It should be stressed that `carlomat` has been designed first of all to deal with reactions involving heavy, unstable particles and it is not particularly well suited for multijet QCD processes, mainly because of the explicit treatment of the color degrees of freedom. Actually, one may encounter problems with a very long computation time already when

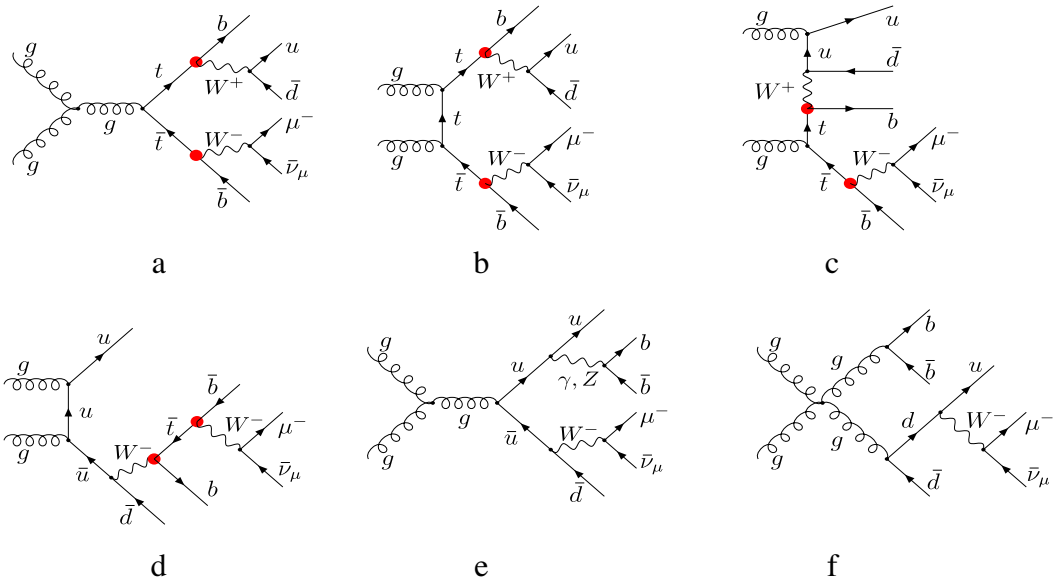

Fig. 1. Examples of the leading order Feynman diagrams of process (1). Blobs indicate the *Wtb* coupling.

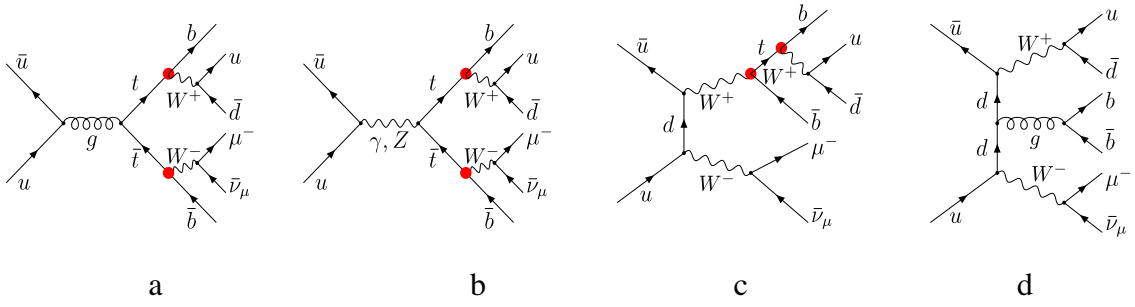

Fig. 2. Examples of the leading order Feynman diagrams of process (2). Blobs indicate the *Wtb* coupling.

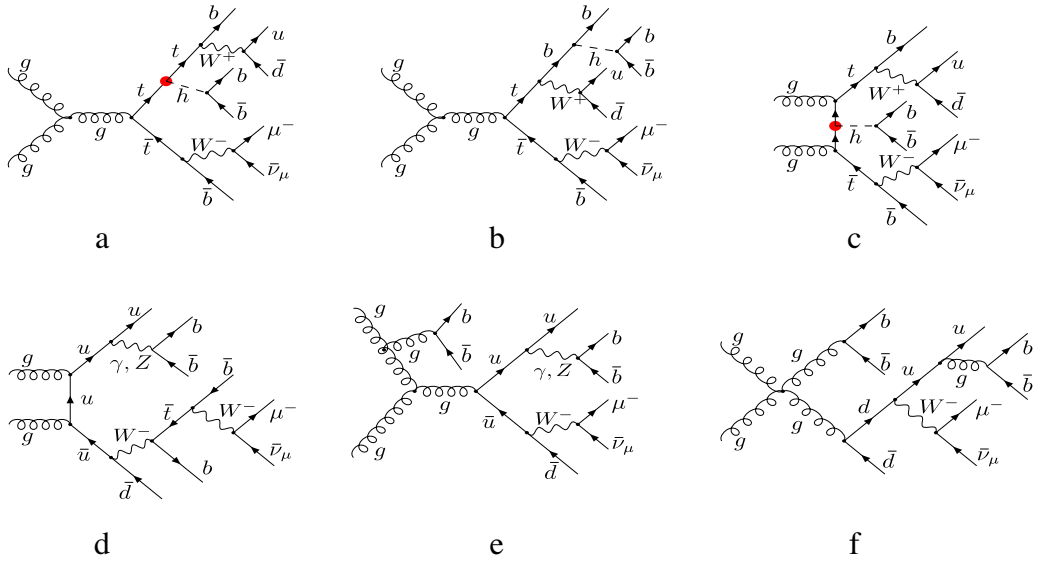

Fig. 3. Examples of the lowest order Feynman diagrams of reaction (3): (a)–(c) are the signal diagrams of $t\bar{t}h$ production, (d)–(f) are the $t\bar{t}h$ background contributions. Blobs indicate the higgs–top coupling.

approaching processes of the proton–proton scattering into 5 or more jets, e.g., computation time of the color matrix for $q\bar{q} \to 5g$ with an Intel Xeon 3 GHz processor is about 2 h, while for $gg \to 5g$ it is estimated to be about 200 h. Moreover, sizes of the arrays generated in the calculations approach typical compiler limits. Therefore, such processes should be much better handled with those of the above listed programs which use the MC summing over colors.

2. Basic changes in the program

In the following, the substantial changes in the program are described.

2.1. Phase space integration

The MC phase space integration in `carlomat` is performed with the use of a multichannel approach which is chosen because the number of peaks in the squared matrix element, that should be mapped out in order to improve convergence of the integral, usually by far exceeds the number of independent variables in a single parameterization of the phase space element given by Eqs. (17) and (19) of [1]. The peaks arise whenever the denominator of a propagator in any of the Feynman diagrams is approaching its minimum. In version 1 of the program, a separate phase space parameterization is generated for each Feynman diagram whose peaks are smoothed with appropriate mappings of the integration variables. A user specified number of individual phase space parameterizations are combined into a kinematical subroutine and then all the subroutines are combined into a single multichannel integration routine, as described in Section 2.4 of [1]. The number should be chosen so as to possibly minimize the compilation time which, however, may be quite long for multiparticle processes with a large number of Feynman diagrams.

An improvement of the phase space integration in the current version of the program is based on a simple observation that the Feynman diagrams of the same topology differ from each other only in propagators of the internal particles. This means that the integration limits of all the variables in phase space parameterizations corresponding to diagrams of the same topology are common and can be written only once. The same holds for the Lorentz boosts of four-momenta of the final state particles. The final state particles are divided into subsets that are characteristic for the topology. Their four-momenta are randomly generated in the relative center of mass frame of the subset and then boosted to the rest frame of the parent subset, and so on until they reach the center of mass frame of all the final state particles.

In order to illustrate this procedure let us consider the diagram of reaction (3) depicted in Fig. 3(a). The final state particles are divided into two subsets: $\{\{b, \bar{b}\}, \{b', \{u, \bar{d}\}\}\}$ and $\{\bar{b}', \{\mu^-, \bar{\nu}_\mu\}\}$, where a prime has been introduced in order to distinguish between the identical quarks in the diagram. The distinction makes sense, as there are 3 other dedicated phase space parameterizations for the diagrams that differ from the one of Fig. 3(a) by the exchanges: $b \leftrightarrow b'$ and/or $\bar{b} \leftrightarrow \bar{b}'$. Note that the diagram of Fig. 3(b), despite having the same shape as that of Fig. 3(a), belongs to a different topology in a sense described in Section 2.1 of [1]. Let us consider the subset $\{\{b, \bar{b}\}, \{b', \{u, \bar{d}\}\}\}$ first. The four-momenta p_u and $p_{\bar{d}}$ are randomly generated in the frame, where $\vec{p}_u + \vec{p}_{\bar{d}} = \vec{0}$. The four-momentum $p_{b'}$ is generated in the frame, where $\vec{p}_{b'} + \vec{p}_{\{u,\bar{d}\}} = \vec{0}$ and the four-momenta p_u and $p_{\bar{d}}$ are boosted to this frame. The four-momenta p_b and $p_{\bar{b}}$ are randomly generated in the frame, where $\vec{p}_b + \vec{p}_{\bar{b}} = \vec{0}$. Then p_b, $p_{\bar{b}}$, $p_{b'}$, p_u and $p_{\bar{d}}$ are boosted to the frame, where $\vec{p}_{\{b,\bar{b}\}} + \vec{p}_{\{b',\{u,\bar{d}\}\}} = \vec{0}$. The four-momenta of the second subset $\{\bar{b}', \{\mu^-, \bar{\nu}_\mu\}\}$ are generated analogously, but this time one Lorentz boost less is required. Finally, all the four-momenta of final state particles are boosted to the center of mass frame. Therefore the integration limits and calls to the boost subroutine are written commonly for all the phase space parameterizations corresponding to the Feynman diagrams of the same topology.

As a result of the modifications described above the phase space integration routine becomes shorter and the compilation time is reduced, by a factor 4–5 for multiparticle reactions, compared to the previous version of the program.

2.2. Hadron–hadron collisions

Interfaces to `MSTW` [11] and `CTEQ6` [12] parton density functions (PDFs) are added in the MC computation part of the program. The user should choose if she/he wants to calculate the cross section of the hard scattering process at the fixed center of mass energy, or to fold it with the parton density functions, treating the initial state particles as partons of either the $p\bar{p}$ or pp scattering. This is controlled by a single flag `ihad` in the main program of the MC computation `carlocom.f`. The choice between the two supported PDF sets is controlled with a flag `ipdf`. The program will automatically assign integer numbers to the initial state partons according to the convention of either `MSTW` or `CTEQ6`. The user should also choose a value of `iset` for the selected PDFs, with a recommended value `iset=0` (the central PDF set) for `MSTW` and `iset=3` (the leading order partons and $\alpha_s(m_Z) = 0.118$) for `CTEQ6`. Moreover, a character variable `prefix` that defines the fit order and location of the grid files must be specified for `MSTW` PDFs.

It is also possible to choose one of 3 predefined factorization scales `Q` by specifying a value of `iscl`:
`iscl=1 (Q=sclf*sqrt(s'))/2 (Q = sclf)/3 (Q=sclf* sqrt(mt**2+sum of ptj**2))`,
where `sclf` is an arbitrary real (double precision) value. The user can easily define other scales by changing the defining expressions for `qsc` in `croskk.f`.

In order to avoid a mismatch of parameters, the quark masses, the minimum value of Bjorken x and a value of $\alpha_s(m_Z)$ are transferred from common blocks `mstwCommon` of `MSTW`, or `XQrange` and `Masstbl` of `CTEQ6` with a single call to either `mstw_interface` or `ctq6f_interface` from a subroutine `parfixkk` after they have been initialized with a call to `GetAllPDFsAlt` or `SetCtq6(iset)`.

If the initial state partons $p_1, p_2 = 0, \pm1, \pm2, \pm3, \pm4, \pm5$ differ from each other then two contributions to the cross section from $(p_1(x_1), p_2(x_2))$ and $(\mp p_2(x_1), \mp p_1(x_2))$, where "$-(+)$" corresponds to proton–proton (proton–antiproton) scattering, are added in a function `crosskk`. On the other hand, a sum over different partonic initial states that lead to the same final state, except for the parton interchange just discussed, is not done automatically in `carlomat`. This is because the program generates a dedicated phase space integration routine that takes into account Feynman diagram topologies and peaks which obviously may be different for some underlying partonic processes of a considered process. Thus contributions from all the underlying partonic processes should be calculated separately and then they can be added, e.g. with a program `addbs` that is appended in directory `test_output`.

2.3. Color matrix

The color matrix in `carlomat` is calculated numerically from the very definition, using explicit expressions for the SU(3) group structure constants and the Gell-Mann matrices, after its size has been reduced with the help of some basic SU(3) algebra properties. In version 1.0 of `carlomat`, the reduced color matrix was cast in a single subroutine `colsqkk.f` that was compiled together with all the other subroutines of the MC program and calculated anew every time the program was run. This posed no problem for processes with a simple color structure, but it unnecessarily increased the computation time for processes with a big size color matrix.

Compilation of the large subroutine containing the entire color matrix was very time consuming, therefore, in the current version of the program, a subroutine `colsqkk.f` is divided into smaller subroutines of the user controlled size which allows us to compile much larger color matrices and speeds up the compilation process.

Moreover, computation of the color matrix is performed as a separate stage, that is automatically executed just after the code generation. Then the resulting nonzero elements of the color matrix and their labels are transferred to the directory, where they are read from subroutine `mpol2.f` of the MC program when it is executed for the first time.

2.4. Cabibbo–Kobayashi–Maskawa mixing

The CKM mixing in the quark sector is implemented in the program. The CKM mixing would be an unnecessary complication for many applications, therefore, an option has been included in `carlomat.f` that allows us to switch it on or off: `ickm=1(yes)/else(no)`.

For the sake of simplicity, only the magnitudes of the CKM matrix elements V_{ij} [13] are taken into account. However, the complex phase of the CKM matrix can be easily incorporated, as the W boson coupling to fermions that always multiplies V_{ij} is complex. To do so, it is enough to change the type of V_{ij} in `inprms.f` to complex and make a distinction between the $Wf\bar{f}'$ couplings and their conjugates in `vertices.dat.ckm`. The latter is a new data file that must be present in directory `code_generation` together with `vertices.dat` that defines the couplings in the absence of the CKM mixing.

If the CKM mixing is included then the numbers of Feynman diagrams of reactions (1) and (2) in the unitary gauge of SM, with the neglect of the Higgs boson coupling to fermions lighter than c-quark, increase to 596 and 1444, respectively.

2.5. Anomalous Wtb coupling

The top quark mass is close to the energy scale of the EW symmetry breaking. Therefore it is possible that the top quark coupling to the W-boson differs from the $V-A$ form of SM. The Wtb coupling is present in any process of the top quark production if a top quark decay in the dominant Wb channel is taken into account. Not only does it enter the signal Feynman diagrams of the top quark production and decay, but it is present also in many other diagrams of the off resonance background contributions to the top quark production. This is illustrated in Figs. 1 and 2, where the Wtb coupling is indicated by red blobs.

The effective Lagrangian of the Wtb interaction containing operators of dimensions four and five that is implemented in the current version of the program has the following form [14]:

$$\begin{aligned} L_{Wtb} = {} & \frac{g}{\sqrt{2}} V_{tb} \left[W^-_\mu \bar{b}\, \gamma^\mu \left(f_1^L P_L + f_1^R P_R\right) t \right. \\ & \left. - \frac{1}{m_W} \partial_\nu W^-_\mu \bar{b}\, \sigma^{\mu\nu} \left(f_2^L P_L + f_2^R P_R\right) t \right] \\ & + \frac{g}{\sqrt{2}} V^*_{tb} \left[W^+_\mu \bar{t}\, \gamma^\mu \left(\bar{f}_1^L P_L + \bar{f}_1^R P_R\right) b \right. \\ & \left. - \frac{1}{m_W} \partial_\nu W^+_\mu \bar{t}\, \sigma^{\mu\nu} \left(\bar{f}_2^L P_L + \bar{f}_2^R P_R\right) b \right], \end{aligned} \tag{4}$$

where g is the weak coupling constant, V_{tb} is the element of the CKM matrix, m_W is the mass of the W boson, $P_{R/L} = \frac{1}{2}(1 \pm \gamma_5)$ are the chirality projectors, $\sigma^{\mu\nu} = \frac{i}{2}[\gamma^\mu, \gamma^\nu]$ and $f_i^L, f_i^R, \bar{f}_i^L, \bar{f}_i^R$, $i = 1, 2$, are form factors which can be complex in general. The SM Wtb interaction is reproduced if $f_1^L = \bar{f}_1^L = 1$ and all the remaining form factors are set to 0.

The implementation of the right-handed vector coupling is straightforward, as it is present in the neutral current interaction SM vertices $f\bar{f}Z$ and $f\bar{f}\gamma$. However, the tensor couplings of (4) are not present in the SM and require new routines for calculating the corresponding helicity matrix elements. Therefore, a routine library `carlolib` has been supplemented with the following new subroutines: `btwan`, `btwmd`, `bwtan`, `bwtmd`, `tbwan`, `tbwmd`, `wbtan`, `wbtmd`, `fefan`, `ffvan`, `fvfan`, and `vffan`. They allow us to calculate all the helicity amplitudes that are necessary for computing cross sections of any process involving the anomalous Wtb coupling defined by (4) and the lowest order top quark width Γ_t which enters the top quark propagator through the complex mass parameter defined in Eq. (13) of [1]. If CP is conserved then the following relationships between the form factors of (4) hold:

$$\bar{f}_1^{R*} = f_1^R, \qquad \bar{f}_1^{L*} = f_1^L, \qquad \bar{f}_2^{R*} = f_2^L, \qquad \bar{f}_2^{L*} = f_2^R. \tag{5}$$

Γ_t is calculated anew, every time the form factors $f_i^L, f_i^R, \bar{f}_i^L$ and $\bar{f}_i^R$, $i = 1, 2$, are changed. It should be stressed that for CP-odd choices of the form factors, i.e., if they do not satisfy (5), the widths Γ_t of t and $\Gamma_{\bar{t}}$ of $\bar{t}$ differ from each other. Thus, both widths are calculated and the following rule is applied to substitute the width in the s-channel top quark propagator: Γ_t is used if the propagator goes into W^+b and $\Gamma_{\bar{t}}$ is used if the propagator goes into $W^-\bar{b}$. The rule does not work for the propagators in the t- or u-channels, but the actual value of the top quark width should not play much of a role in them.

A new version of `carlomat` allows us to make predictions for the top quark production and decay in hadronic collisions, through different underlying partonic processes, while taking into account complete sets of the lowest order Feynman diagrams and full information on spin correlations between the top quark and its decay products. It was used to obtain theoretical predictions in the presence of anomalous Wtb coupling for the forward–backward asymmetry in top quark pair production at the Tevatron [15] and for distributions of μ^- in the top quark pair production reaction $pp \to bu\bar{d}\bar{b}\mu^-\bar{\nu}_\mu$ at the LHC [16]. It can also be applied for studying anomalous effects in the top quark production and decay in e^+e^- collisions at a linear collider [17,18], as it was done before with "hand made" modifications of a program `eett6f` [19].

2.6. Anomalous top–Higgs Yukawa coupling

Due to the large top quark mass, the top–Higgs Yukawa coupling

$$g_{t\bar{t}h} = m_t/v, \quad \text{with } v = (\sqrt{2}G_F)^{-1/2} \simeq 246 \text{ GeV}, \tag{6}$$

is by far the biggest Yukawa coupling of SM. Its measurement, which may bring hints towards a better understanding of the EW symmetry breaking mechanism of the SM, will certainly be one of the key points in the study of a profile of recently discovered candidate for the Higgs boson [20].

The most general Lagrangian of $t\bar{t}h$ interaction including corrections from dimension-six operators that has been implemented in the program has the following form [21]

$$\mathcal{L}_{t\bar{t}h} = -g_{t\bar{t}h}\bar{t}\left(f + if'\gamma_5\right) th, \tag{7}$$

where f and f' that describe the scalar and pseudoscalar departures, respectively, from a purely scalar top–Higgs Yukawa coupling $g_{t\bar{t}h}$ of SM are assumed to be real. The top–Higgs Yukawa coupling of SM is reproduced in Eq. (7) for $f = 1$ and $f' = 0$.

Implementation of the general coupling of Eq. (7) in the program was relatively easy, as in the complex mass scheme [22], the coupling $g_{t\bar{t}h}$ is of the complex type. It is parameterized in `carlomat` in the following way:

$$g_{t\bar{t}h} = e_W \frac{M_t}{2\sin\theta_W M_W}, \tag{8}$$

where complex masses M_t and M_W are defined in Eq. (13) of [1], and the complex EW mixing parameter $\sin\theta_W$ is defined in Eq. (14)

of [1]. The electric charge e_W of Eq. (8) that enters multiplicatively all the EW couplings can be defined as either a real or complex quantity, by selecting an appropriate value of a flag `ialpha` in `carlocom.f`.

If we now write Lagrangian (7) in the form

$$\mathcal{L}_{t\bar{t}h} = -\bar{t}\left(f^{(R)}_{t\bar{t}h}P_R + f^{(L)}_{t\bar{t}h}P_R\right) th \tag{9}$$

and take into account the form of the γ_5 and $P_{R/L} = \frac{1}{2}(1 \pm \gamma_5)$ matrices in the Weyl representation:

$$\gamma_5 = \begin{pmatrix} -\mathbb{I} & 0 \\ 0 & \mathbb{I} \end{pmatrix}, \qquad P_R = \begin{pmatrix} 0 & 0 \\ 0 & \mathbb{I} \end{pmatrix}, \qquad P_L = \begin{pmatrix} -\mathbb{I} & 0 \\ 0 & 0 \end{pmatrix}, \tag{10}$$

where $\mathbb{I}$ is a 2×2 unit matrix, then we will immediately see that

$$f^{(R)}_{t\bar{t}h} = g_{t\bar{t}h}\left(f + if'\right), \qquad f^{(L)}_{t\bar{t}h} = g_{t\bar{t}h}\left(f - if'\right). \tag{11}$$

As the SM Lagrangian of the top–Higgs Yukawa interaction in `carlomat` has the same form as Lagrangian (9) with $f^{(R)}_{t\bar{t}h} = f^{(L)}_{t\bar{t}h} = g_{t\bar{t}h}$, substitutions (11) are practically the only change that are required in the program.

The current version of `carlomat` was used in [23] to study effects of the anomalous $t\bar{t}h$ coupling of Eq. (7) on the differential distributions in rapidity and angles of the μ^- in the reaction $pp \to bu\bar{d}\bar{b}\mu^-\bar{\nu}_\mu b\bar{b}$ which is one of the channels of associated production of the top quark pair and Higgs boson in proton–proton collisions at the LHC. The dominant contribution to the reaction comes from the underlying gluon–gluon fusion partonic process (3) examples of the Feynman diagrams of which are shown in Fig. 3, where the coupling corresponding to Lagrangian (7) has been indicated with a blob.

2.7. Scalar electrodynamics

The knowledge of energy dependence of the total cross section of electron–positron annihilation into hadrons $\sigma_{e^+e^-\to\text{hadrons}}(s)$ allows, through dispersion relations, for determination of hadronic contributions to the vacuum polarization, which in turn are necessary for improving precision of theoretical predictions for the muon anomalous magnetic moment and play an important role in the evolution of the fine structure constant from the Thomson limit to high energy scales. Theoretical predictions for $\sigma_{e^+e^-\to\text{hadrons}}(s)$ within quantum chromodynamics are possible only in the perturbative regime of the theory, i.e. in the high energy range, where due to the asymptotic freedom, the strong coupling constant is small. In the energy range below the J/ψ threshold, $\sigma_{e^+e^-\to\text{hadrons}}(s)$ must be measured, either by the initial beam energy scan or with the use of a radiative return method [24]. The idea behind the method is that the actual energy of e^+e^- scattering in the radiative reaction $e^+e^- \to \text{hadrons} + \gamma$ becomes smaller if a hard photon is emitted off the initial electron or positron prior to their annihilation. Thus, if the hard photon energy is measured and the photon emission off the final state hadrons is properly modeled, it is possible to determine the cross section of $e^+e^- \to$ hadrons at the reduced energy from the corresponding radiative process being measured at a fixed energy in the center of mass system. At low energies, such radiative hadronic final states consist mostly of pions, accompanied by one or more photons.

The scalar quantum electrodynamics (sQED) is a theoretical framework that allows us to describe effectively the low energetic electromagnetic interaction of charged pions. Despite being bound states of the electrically charged quarks, at low energies, $\pi^\pm$ can be treated as pointlike particles and represented by a complex scalar field φ. The $U(1)$ gauge invariant Lagrangian of sQED that is implemented in `carlomat` has the following form:

$$\mathcal{L}^{\text{sQED}}_\pi = \partial_\mu\varphi\,(\partial^\mu\varphi)^* - m^2_\pi\varphi\varphi^* - ie\left(\varphi^*\partial_\mu\varphi - \varphi\partial_\mu\varphi^*\right)A^\mu + e^2 g_{\mu\nu}\varphi\varphi^* A^\mu A^\nu. \tag{12}$$

The corresponding Feynman rules can be found, e.g., in [25]. The bound state nature of the charged pion is taken into account by the substitutions:

$$e \to eF_\pi(q^2), \qquad e^2 \to e^2\left|F_\pi(q^2)\right|^2,$$

where $F_\pi(q^2)$ is the charged pion form factor [25]. Both three- and four-point interactions are included in the program, but a formula for the form factor has not yet been implemented.

3. Other changes and preparation for running

Other minor changes to the program, including corrections of a few bugs are described in a `readme` file.

`carlomat v. 2.0` is distributed as a single `tar.gz` archive `carlomat_2.0.tgz`. After executing a command
`tar -xzvf carlomat_2.0.tgz`
directory `carlomat_2.0` will be created.
For the user's convenience files `mstwpdf.f` of `MSTW` and `Ctq6Pdf.f` and `cteq6l.tbl` of `CTEQ6` are included in the current distribution of `carlomat`. To put `MSTW` grid files on your computer download a file `mstw2008grids.tar.gz` from
http://mstwpdf.hepforge.org/code/code.html
and unpack the tarball with
`tar -xzvf mstw2008grids.tar.gz`
in the same directory where `carlomat_2.0.tgz` was unpacked.

In order to prepare the program for running take the following steps:

- select a Fortran 90 compiler in `makefile`'s of `code_generation` and `mc_computation`, which need not be the same, and compile all the routines stored in `carlolib` with the same compiler as that chosen in `mc_computation`;
- go to `code_generation`, specify the process and necessary options in `carlomat.f` and execute `make code` from the command line.

Once the code generation is finished, the color matrix is compiled and computed. The control output files `test` and `test_clr` in `code_generation` should reproduce the delivered files `test_gg` and `test_clr_gg` for process (1) or `test_uu` and `test_clr_uu` for process (2). Then

- go to `mc_computation`, choose the required options and the center of mass energy by editing properly `carlocom.f` and execute `make mc` in the command line.

When the run is finished all output files are automatically moved to directory `test_output`. They should reproduce the files delivered in directory `test_output0`. The basic output of the MC run is stored in a file whose name starts with `tot`. Files with prefixes `db` and `dl` contain data for making plots of differential cross sections with boxes and lines, respectively, with the use of `gnuplot`. The distributions of processes with different initial state partons can be added with the help of a simple program `addbs` appended in directory `test_output`. The program should be appropriately edited, compiled and run twice in order to add distributions stored in files with prefixes `db` and `dl`. An example of the input file `example.plo` for `gnuplot` is also appended in

`test_output`. The distributions can be plotted and viewed with a command:
`make plot`.

The user can define his/her own distributions by modifying appropriately files `calcdis.f` and `distribs.f` in directory `mc_computation`.

Note that whenever the Fortran compiler in `mc_computation` is changed, or a compiled program is transferred from a machine with different architecture, then all the object and module files in the directory should be deleted by executing the commands:
`rm *.o`
`rm *.mod`
and all the Fortran files in `carlolib` should be compiled anew.

Acknowledgments

This project was supported in part with financial resources of the Polish National Science Centre (NCN) under grant decision number DEC-2011/03/B/ST6/01615 and by the Research Executive Agency (REA) of the European Union under the Grant Agreement number PITN-GA-2010-264564 (LHCPhenoNet).

References

[1] K. Kołodziej, Comput. Phys. Comm. 180 (2009) 1671;
K. Kołodziej, Acta Phys. Polon. B 42 (2011) 2477.
[2] T. Stelzer, W.F. Long, Comput. Phys. Comm. 81 (1994) 357;
F. Maltoni, T. Stelzer, J. High Energy Phys. 02 (2003) 027;
J. Alwall, M. Herquet, F. Maltoni, O. Mattelaer, T. Stelzer, J. High Energy Phys. 06 (2011) 128;
H. Murayama, I. Watanabe, K. Hagiwara, KEK-91-11.
[3] A. Pukhov, et al. arXiv:hep-ph/9908288;
E. Boos, et al., Nucl. Instrum. Methods A 534 (2004) 250;
A. Belyaev, N.D. Christensen, A. Pukhov, Comput. Phys. Comm. 184 (2013) 1729.
[4] M.L. Mangano, M. Moretti, F. Piccinini, R. Pittau, A. Polosa, J. High Energy Phys. 0307 (2003) 001.
[5] A. Kanaki, C.G. Papadopoulos, Comput. Phys. Comm. 132 (2000) 306;
C.G. Papadopoulos, Comput. Phys. Comm. 137 (2001) 247;
A. Cafarella, C.G. Papadopoulos, M. Worek, Comput. Phys. Comm. 180 (2009) 1941.
[6] T. Gleisberg, et al., J. High Energy Phys. 0402 (2004) 056;
T. Gleisberg, et al., J. High Energy Phys. 0902 (2009) 007;
T. Gleisberg, S. Höche, J. High Energy Phys. 0812 (2008) 039.
[7] M. Moretti, T. Ohl, J. Reuter, arXiv:hep-ph/0102195;
W. Kilian, T. Ohl, J. Reuter, Eur. Phys. J. C 71 (2011) 1742.
[8] J. Küblbeck, M. Böhm, A. Denner, Comput. Phys. Comm. 60 (1990) 165;
T. Hahn, Nucl. Phys. Proc. Suppl. 89 (2000) 231;
T. Hahn, Comput. Phys. Comm. 140 (2001) 418.
[9] H. Tanaka, T. Kaneko, Y. Shimizu, Comput. Phys. Comm. 64 (1991) 149;
F. Yuasa, et al., Progr. Theoret. Phys. Suppl. 138 (2000) 18;
G. Belanger, et al., Phys. Rep. 430 (2006) 117.
[10] G. Bevilacqua, et al., Comput. Phys. Comm. 184 (2013) 986.
[11] A.D. Martin, W.J. Stirling, R.S. Thorne, G. Watt, Parton distributA, Eur. Phys. J. C 63 (2009) 189–285.
[12] J. Pumplin, et al., J. High Energy Phys. 07 (2002) 012.
[13] J. Beringer, et al., Particle Data Group, Phys. Rev. D 86 (2012) 010001.
[14] G.L. Kane, G.A. Ladinsky, C.-P. Yuan, Phys. Rev. D 45 (1992) 124.
[15] K. Kołodziej, Phys. Lett. B 710 (2012) 671, arXiv:1110.2103.
[16] K. Kołodziej, Acta Phys. Pol. B44 (2013) 1775, arXiv:1212.6733.
[17] James Brau, Yasuhiro Okada, Nicholas Walker, et al. [ILC Reference Design Report Volume 1—Executive Summary], arXiv:0712.1950;
J.A. Aguilar-Saavedra, et al. [ECFA/DESY LC Physics Working Group Collaboration], arXiv:hep-ph/0106315;
T. Abe, et al. [American Linear Collider Working Group Collaboration], arXiv:hep-ex/0106056;
K. Abe, et al. [ACFA Linear Collider Working Group Collaboration], arXiv:hep-ph/0109166.
[18] R.W. Assmann, et al. [CLIC Study Team], CERN 2000-008;
H. Braun, et al. [CLIC Study Group], CERN-OPEN-2008-021, CLIC-Note-764.
[19] K. Kołodziej, Phys. Lett. B 584 (2004) 89;
K. Kołodziej, Comput. Phys. Comm. 151 (2003) 339.
[20] ATLAS Collaboration, Phys. Lett. B 716 (2012) 1;
CMS Collaboration, Phys. Lett. B 716 (2012) 30.
[21] J.A. Aguilar-Saavedra, Nuclear Phys. B 821 (2009) 215. arXiv:0904.2387.
[22] A. Denner, S. Dittmaier, M. Roth, D. Wackeroth, Nuclear Phys. B560 (1999) 33. Comput. Phys. Comm. 153 (2003) 462.
[23] K. Kołodziej, J. High Energy Phys. 07 (2013) 083, arXiv:1303.4962.
[24] Min-Shih Chen, P.M. Zerwas, Phys. Rev. D 11 (1975) 58.
[25] F. Jegerlehner, The Anomalous Magnetic Moment of the Muon, Springer, ISBN: 9783540726333, 2007.